Chaotic mixing in thermocapillary-driven microdroplets

Roman O. Grigoriev[a)]
School of Physics, Georgia Institute of Technology, Atlanta, Georgia 30332-0430

(Received 17 June 2004; accepted 16 November 2004; published online 4 February 2005)

Liquid microdroplets represent a convenient system for studies of mixing by chaotic advection in discrete microscopic volumes. The mixing properties of the flows in microdroplets are governed by their symmetries, which give rise to invariant surfaces serving as barriers to transport. Thorough mixing via chaotic advection requires destruction of all such invariant surfaces. To illustrate this idea, we demonstrate that quick and thorough mixing inside a spherical microdroplet suspended in a layer of substrate fluid can be obtained by moving the droplet along a two-dimensional path using temperature-induced surface tension gradients. The use of flow invariants also provides a convenient way to analyze the mixing properties of flows in many other experimental implementations. © *2005 American Institute of Physics*. [DOI: 10.1063/1.1850374]

I. INTRODUCTION

Most microfluidic systems, which are being developed into "labs-on-a-chip" that promise revolutionary applications in biotechnology, chemistry, and medicine,[1–4] require efficient mixing of initially distinct fluid volumes. Liquids, however, do not mix easily at the scale of typical microfluidic devices. Physically, microscale flows are characterized by a low Reynolds number $\mathrm{Re} \equiv Va/\nu < 1$, where V and a are, respectively, a characteristic flow speed and length, and ν is the liquid's kinematic viscosity. In this regime, flows are laminar, and turbulence, which governs mixing rates in macroscopic systems, cannot arise. Yet the size of typical microfluidic devices is too large for molecular diffusion, which usually governs mixing at smaller scales, to become effective. Thus, efficient mixing of liquids at the microscale requires a stirring mechanism, such as chaotic advection,[5,6] that stretches and folds fluid elements throughout the entire volume of the flow. The folding leads to a decrease in the average distance between unmixed volumes of liquid with different composition, while stretching sharpens the concentration gradients enhancing diffusion, which acts more rapidly to smooth out remaining nonuniformities. For devices based on continuous flow through microchannels, strategies for inducing chaotic mixing by altering device geometries have been proposed and verified experimentally.[7,8]

Our focus here will be on discrete volume systems[4,9–11] which allow miniaturization of many standard laboratory protocols that are difficult to realize with continuous flow. We will concentrate primarily on spherical volumes, such as microdroplets of one liquid suspended in another liquid, both because such configurations are easy to implement and study experimentally and because the flows inside spherical volumes can be computed analytically due to the high symmetry of the problem. This high symmetry, coupled with the time-reversal invariance of the Stokes (low-Re) flow, proves to be a mixed blessing as it also makes designing a chaotic microflow with good mixing properties a lot more challenging than in the case of unbounded geometries.

The layout of the paper is as follows. Section II summarizes prior theoretical and experimental developments in the field. Section III describes the procedure for computing the flow inside the droplet in the proposed experimental setup. Section IV contains the analysis of the mixing properties of the flow. Finally, the conclusions are presented in Sec. V.

II. BACKGROUND

The three most common flows that arise in spherical microdroplets are the Hill's spherical vortex (or "dipole") flow, the axisymmetric extensional (or "quadrupole") flow, and the Taylor (or "rolling") flow. Specifically, the dipole flow (Fig. 1) describes the flow inside a viscous droplet undergoing translational motion due to buoyancy,[12] thermocapillary effect,[13] or nonuniform electric field.[14] The corresponding velocity field is given (in the frame of the drop) by

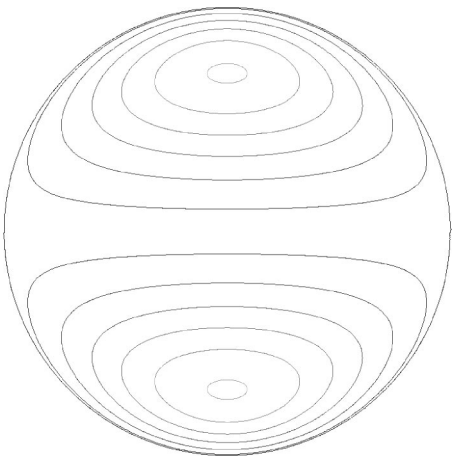

FIG. 1. Streamlines of the dipole flow at the midplane of the droplet. Vector **e** is in the horizontal direction.

[a)]Electronic mail: roman.grigoriev@physics.gatech.edu

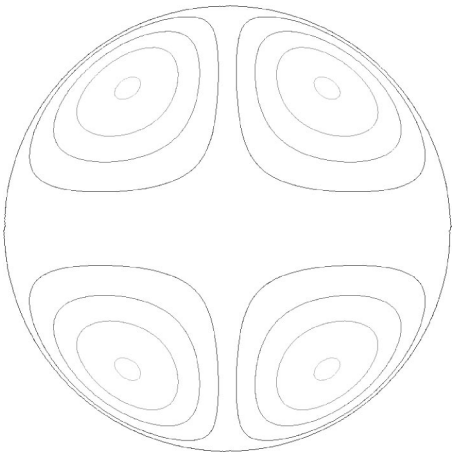

FIG. 2. Streamline of the quadrupole flow at the midplane of the droplet. Vector **e** is in the horizontal direction.

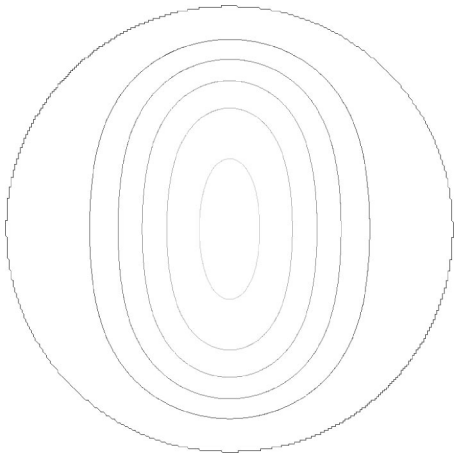

FIG. 3. Streamlines of the Taylor flow at the midplane of the droplet. Vectors $\mathbf{e}_1$ and $\mathbf{e}_2$ are in the horizontal and vertical direction, respectively. In this example $\lambda=1$.

$$\mathbf{v}_d = V_d[(\mathbf{e}\cdot\mathbf{r})\mathbf{r} - (2r^2-1)\mathbf{e}], \tag{1}$$

where **e** is a unit vector defining the orientation of the axis of the flow, V_d is the characteristic velocity, and all coordinates have been nondimensionalized by the droplet diameter a. The quadrupole flow (Fig. 2)

$$\mathbf{v}_q = V_q[(r^2+2(\mathbf{e}\cdot\mathbf{r})^2-1)\mathbf{r} - (5r^2-3)(\mathbf{e}\cdot\mathbf{r})\mathbf{e}], \tag{2}$$

with characteristic velocity V_q, can be induced by placing the droplet in an axisymmetric extensional flow[15] $\hat{\mathbf{v}}^\infty \propto \mathbf{r} - 3(\mathbf{e}\cdot\mathbf{r})\mathbf{e}$, or subjecting it to a uniform electric field.[16] Here $\hat{\mathbf{v}}^\infty$ denotes the flow far from the droplet and the unit vector **e** again defines the axial direction. Finally, the velocity field obtained by placing the droplet in a shear flow $\hat{\mathbf{v}}^\infty \propto (\mathbf{e}_1\cdot\mathbf{r})\mathbf{e}_2$, with $\mathbf{e}_1$ and $\mathbf{e}_2$ two orthogonal unit vectors, is a special case of the flow computed by Taylor[15] and takes the form

$$\mathbf{v}_t = V_t[(5r^2-3)\{(\mathbf{e}_1\cdot\mathbf{r})\mathbf{e}_2 + (\mathbf{e}_2\cdot\mathbf{r})\mathbf{e}_1\} - 4(\mathbf{e}_1\cdot\mathbf{r})(\mathbf{e}_2\cdot\mathbf{r})\mathbf{r} + 2(1+\lambda)(\mathbf{e}_1\times\mathbf{e}_2)\times\mathbf{r}], \tag{3}$$

where $\lambda=\mu/\hat{\mu}$ is the ratio of inside to outside fluid dynamic viscosities and V_t is again the characteristic velocity of the flow (Fig. 3). In the limit $\lambda\to\infty$ this flow reduces to a rigid body rotation of the droplet around the axis $\mathbf{e}_1\times\mathbf{e}_2$.

If one neglects diffusion, the advection becomes the only transport mechanism, so the trajectories of infinitesimal fluid volumes with different composition are described by the flow

$$\dot{\mathbf{r}} = \mathbf{v}(\mathbf{r},t). \tag{4}$$

The mixing properties of the flow are therefore defined by the geometrical properties of the invariant sets of the dynamical system (4). The high degree of geometrical symmetry of many typical flows leads to the existence of flow invariants (or actions in the language of Hamiltonian systems[17]), which are functions of coordinates that are constant along streamlines of the flow. Each invariant defines, inside the volume of droplet, surfaces on which the flow is effectively two-dimensional. Additional invariants further reduce the flow dimensionality; e.g., a steady flow with two invariants is effectively one dimensional.

Most of the theoretical progress in understanding chaotic mixing in bounded flows has been achieved via studies of *weakly perturbed* steady integrable flows. These flows are structurally unstable: arbitrarily small perturbations can lead to chaos. The effect of small perturbations can be included using standard perturbation analysis based on averaging their contribution over a period of the unperturbed trajectories.[17–22] However, small perturbations only lead to weak nonintegrability. For instance, perturbed two-invariant (or action-action-angle) flows, such as the axisymmetric flows (1) and (2), generically possess an adiabatic invariant (AI). The value of the AI slowly drifts due to intersection of constant-AI tori with surfaces on which the frequency of the angle variable vanishes (e.g., separatrices of the unperturbed flow) or satisfies a resonance condition.[23] As a result, the chaotic trajectories can explore large three-dimensional regions, but only on extremely long time scales. On the other hand, single-invariant (or action-angle-angle) flows, such as an axisymmetric flow superimposed with rotation around the axis,[20] represent motion on nested tori, with generic perturbations leading to breakup of the resonant KAM-like tori (KAM—Kolmogorov–Arnold–Moser). Therefore, in weakly perturbed action-angle-angle flows mixing occurs only inside thin shells bounded by the undestroyed tori and as such is also quite ineffective.

Time-periodic flows have received comparatively little attention.[23–25] Again the progress in fundamental understanding of their mixing properties is limited to perturbative and numerical studies. As the above discussion suggests, for both steady and time-dependent flows quick and thorough mixing inside the droplet is expected to require *nonperturbative* corrections (i.e., superposition of two or more integrable flows with different symmetries and similar strength). To date, theoretical studies of nonperturbative effects have been limited to numerical simulations.[20,21,25,26]

With a single exception provided by the recent experimental investigation by Ward and Homsy,[27] theoretical and experimental research in this area have by and large been completely disconnected. Few of the theoretical investigations mentioned above are of practical significance, as most

of the studied combinations of flows are nearly impossible to realize experimentally. Respectively, the experimental studies of mixing in microdroplets[28–33] have in no way relied on the existing theoretical results.

Although chaos can, in principle, arise in steady three dimensional flows, all experiments, without exception, relied on time-dependent flows to generate chaotic advection. In one group of experiments[29–32] *deformed* microdroplets confined between two flat surfaces were used. Two droplets (one dyed and one undyed) were merged and moved using electrowetting.[29–32] Although detailed studies of the distribution of mixed volumes inside the droplet have not been conducted (the depth-averaged signal has been recorded) it was determined that one dimensional "shaking" of the droplet does not lead to mixing due to the time reversibility of the Stokes flow—moving the droplet to the original position restores the initial (unmixed) state.[29] However, moving the droplet in two dimensions, e.g., around the perimeter of a rectangle,[30,31] appears to mix the dye much better. Similarly, the studies of liquid droplets (or "plugs") confined by microchannels also found that bending the microchannels in two dimensions (and thereby making the flow inside the droplets time-dependent) improves mixing.[33]

A qualitative two-dimensional model was proposed by Fowler *et al.*[31] to explain mixing in droplets moved along square paths (the corresponding experiments were performed with droplets compressed so strongly, they were effectively two dimensional). Without explicitly referencing the chaotic advection mechanism, the authors suggested that motion in a straight line leads to stretching of fluid volumes, while switching the direction of motion leads to folding. This stretching and folding repeated multiple times describes a classical chaotic mixing mechanism leading to fractal structure of chaotic invariant sets.

Stretching and folding of fluid elements in *spherical* droplets has also been demonstrated experimentally,[27] supporting the results of the theoretical analysis[25] conducted earlier. The primary (dipole) flow in the droplet was generated due to its motion as the droplet sank to the bottom of the container. An additional time-dependent quadrupole flow with the same axis was superimposed by applying an alternating vertical electric field. However, the limitations of the experimental setup prevented the thorough mixing of the dye inside the droplet. As we will show below, this is due to the remaining axial symmetry of the flow which restricts all chaotic trajectories to two-dimensional surfaces.

III. FLOW MANIPULATION

As we have seen so far, chaotic advection requires a flow with rather special properties to be induced inside the microdroplet. Even though any linear superposition of Stokes flows satisfies the Stokes equation, the list of "building blocks" is not large, regardless of what physical mechanism is actually used to drive the flow. Detailed experimental studies of different combinations of basic flows, therefore, require considerable flexibility in the experimental setup. Electrical or thermal fields provide arguably the easiest and most flexible way for controlling the flow. Several approaches based on applying the electric field were discussed in the preceding section.

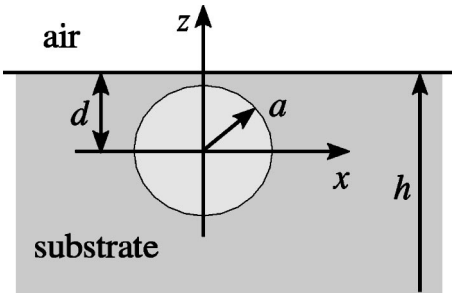

FIG. 4. Microdroplet in a liquid substrate. For convenience we will choose the z axis in the vertical direction and place the origin in the center of the droplet.

Here we describe an alternative approach to driving microflows based on the temperature dependence of surface tension (the Marangoni or thermocapillary effect). Manipulating surface tension provides a natural approach to regulating flows at small scales because surface forces, like surface tension, dominate when the surface-to-volume ratio is large. The surface tension at the interface between immiscible fluids can be conveniently altered by changing the temperature; for pure fluids, the surface tension decreases as the temperature increases. The fluids move when gradients in temperature induce surface tension differences. At small scale, even small thermal gradients can cause substantial fluid movement. As a consequence, the thermocapillary effect has been utilized successfully in prototype devices for manipulating tiny quantities of fluid.[3,4,34] In these devices, temperature variations have been generated with heating/cooling elements (e.g., resistive heaters) placed in physical contact with the fluids. Surface-tension gradients can also be imposed using radiative heating.[35]

In particular, thermocapillary effect can be used to drive the flow inside microdroplets suspended in a layer of liquid substrate (of thickness h, see Fig. 4). In describing the flow inside the droplet subjected to a nonuniform temperature field we will make a number of simplifying assumptions to obtain a tractable analytical model. First of all, we will assume that the droplet is neutrally buoyant and floats a distance $d > a$ below the substrate/air interface and consider the substrate to be semi-infinite (in other words, $h \gg a$). We will assume the droplet to be spherical, which is a good approximation for sufficiently small droplets and the substrate/air interface to be perfectly flat. The surface tension will be assumed to depend linearly on temperature and be independent of the dye concentration. Next, we will assume that the thermal properties of the liquid inside and outside the droplet are the same (this assumption is nonessential and very easy to lift). We will also assume that the convective heat flux is negligible, so the temperature and velocity fields can be computed independently. Finally, the flow is assumed to be in the Stokes regime.

Neglecting the proximity of the substrate/air interface, the velocity inside and outside the droplet can be found by solving the Stokes equation

$$\nabla p = \mu \nabla^2 \mathbf{v}, \quad \nabla \hat{p} = \hat{\mu} \nabla^2 \hat{\mathbf{v}} \tag{5}$$

in an infinite domain subject to the incompressibility condition $\nabla \cdot \mathbf{v} = \nabla \cdot \hat{\mathbf{v}} = 0$ and boundary conditions

$$\mathbf{t} \cdot \mathbf{v} = \mathbf{t} \cdot \hat{\mathbf{v}}, \quad \mathbf{n} \cdot \mathbf{v} = \mathbf{n} \cdot \hat{\mathbf{v}} = 0,$$
$$\mathbf{n} \cdot (\sigma - \hat{\sigma}) \cdot \mathbf{t} = \tau_s (\mathbf{t} \cdot \nabla T) \tag{6}$$

on the surface of the droplet. In the above expressions p, σ, T, and $\tau_s = \partial \gamma_s / \partial T < 0$ denote the pressure, stress tensor, temperature, and temperature coefficient of the surface tension, respectively, the hat denotes the quantities pertaining to the outside liquid, the index s denotes the (spherical) surface of the droplet, and $\mathbf{n}$ and $\mathbf{t}$ are unit vectors normal and tangential to the surface. The velocity field can be found by substituting Lamb's general solution[36] into (6).

As the droplet is constrained to move in the horizontal plane we will only consider the motion arising due to the horizontal component of the temperature gradient. For a uniform gradient $\nabla T = \kappa_0 \mathbf{e}$, the flow inside the droplet can be easily found[13] and is given by (1) with $V_d = \kappa_0 a \tau_s / [\hat{\mu}(2 + 3\lambda)]$. The nonuniformity of the temperature gradient will produce a correction to this basic dipole flow. In particular, for a temperature profile quadratic in the distance from the droplet center, $T = T_0 + \kappa_1 (\mathbf{e} \cdot \mathbf{r})^2$, we find the correction given by the quadrupole flow (2) with $V_q = \kappa_1 a^2 \tau_s / [5\hat{\mu}(1+\lambda)]$.

The proximity of the substrate/air interface will produce additional corrections. First of all, due to the thermocapillary effect at that interface induced by the temperature gradient a shear flow will be established in the liquid substrate. The uniform temperature gradient will induce a uniform (far from the droplet) shear which can be found from the boundary conditions at the substrate/air interface,

$$\mathbf{n} \cdot \hat{\mathbf{v}} = 0, \quad \mathbf{n} \cdot \hat{\sigma} \cdot \mathbf{t} = \tau_p (\mathbf{t} \cdot \nabla T), \tag{7}$$

where $\tau_p = \partial \gamma_p / \partial T < 0$ and the index p denotes the (plane) interface. The corresponding velocity profile in the stationary reference frame is

$$\hat{\mathbf{v}}^{\infty} = \frac{\kappa_0 \tau_p a}{\hat{\mu}} (\mathbf{e}_z \cdot \mathbf{r}) \mathbf{e} + \hat{\mathbf{v}}_0 \mathbf{e}. \tag{8}$$

This shear flow leads to a Taylor flow correction (3) with $V_t = \kappa_0 \tau_p a / [4\hat{\mu}(1+\lambda)]$ and $\mathbf{e}_1 = \mathbf{e}_z$, $\mathbf{e}_2 = \mathbf{e}$. A quick comparison of the characteristic velocities V_d and V_t shows that the shear-induced flow inside the droplet is of roughly the same magnitude as the dipole flow [for $\lambda = O(1)$]. The superposition of these two flows is not chaotic when the vorticity of the shear flow far from the droplet is orthogonal to the axis of the dipole flow, as numerical calculations of Bryden and Brenner[26] show. This is exactly the case here, as the vorticity of the flow (8) is $\omega = \nabla \times \hat{\mathbf{v}}^{\infty} \propto \mathbf{e}_z \times \mathbf{e}$.

The last term in (8) describes the mean flow in the substrate. For a liquid substrate of thickness h the mean flow leads to the overall advection of the droplet in the direction opposite to the temperature gradient with velocity $\hat{\mathbf{v}}_0 = -(\kappa_0 \tau_p / \hat{\mu})(h-d)\mathbf{e}$, which is found using the no-slip boundary condition at the bottom of the substrate layer. For droplets floating near the top interface, $d \ll h$, this motion is dominant compared with the thermocapillary migration[13] with speed $(2/3)V_d$ in the opposite direction.

The proximity of the substrate/air interface will also generate smaller corrections to the flow inside and outside the droplet. Consider, for instance, the flow outside the droplet due to the applied uniform temperature gradient $\nabla T = \kappa_0 \mathbf{e}$. The velocity field in the unbounded substrate again follows from the Lamb's general solution. In the frame of the drop one obtains

$$\hat{\mathbf{v}}_d = -V_d \frac{3(\mathbf{e} \cdot \mathbf{r})\mathbf{r} - r^2 \mathbf{e}}{3r^5}. \tag{9}$$

The solution satisfying the homogeneous version of the boundary conditions (7) at the substrate/air interface can be found using the method of reflections, which generates a series expansion for the velocity field in powers of $\delta = a/d$ by subsequent reflections of the velocity field $\hat{\mathbf{v}}$ about the plane and spherical interface.[37] The leading order corrections are of order δ^3 and so decay very quickly with the distance from the droplet to the interface. Here we will assume that d is large enough for these corrections to be neglibible. The investigation of the effect of these corrections on the mixing properties of the flow will be reported in a separate publication.

One of the principal assumptions in our description concerns the droplet shape. Its deviation from a perfect sphere due to the imposed temperature gradient is given by the ratio of the surface tension variation across the drop, $\Delta\gamma = 2\kappa_0 \tau_s a$, to the mean value of the surface tension γ_s. The temperature gradient κ_0 produced by locally heating the substrate of thickness h to a temperature ΔT above average is of order $\Delta T / h$. Taking the values characteristic of typical fluids and typical experimental conditions, $\gamma_s = 20$ dyn/cm, $\tau_s = 0.1$ dyn/cm K, $\Delta T = 10$ K, and $h = 0.5$ cm we obtain $a \ll h\gamma_s / 2\tau_s \Delta T \approx 5$ cm, so any entirely submerged droplet would be nearly perfectly spherical. In contrast, the influence of terrestrial gravity would be much more pronounced. Comparing the hydrostatic pressure drop $2a\Delta\rho g$ with the Laplace pressure γ_s / a, we obtain $a \ll \sqrt{\gamma_s / 2\Delta\rho g} \approx 0.3$ cm for a typical density mismatch $\Delta\rho = 0.1$ g/cm^3, so only droplets with radii of a few hundred microns or less would be spherical.

IV. TRANSPORT BARRIERS AND MIXING

Having understood the effect of imposed thermal gradients on the motion of and flows inside the droplet, we move on to the mixing problem. The mixing properties of the flows inside the microdroplet are governed by their symmetries, which give rise to invariant surfaces serving as barriers to transport. Since no streamlines of the flow can cross the invariant surfaces, the existence of invariants is highly undesirable in the mixing problem as their presence inhibits complete stirring of the full microdroplet volume by chaotic advection. Thus, the key to achieving effective chaotic mixing in a microdroplet (indeed, in any laminar microflow) is to ensure that all flow invariants are destroyed.

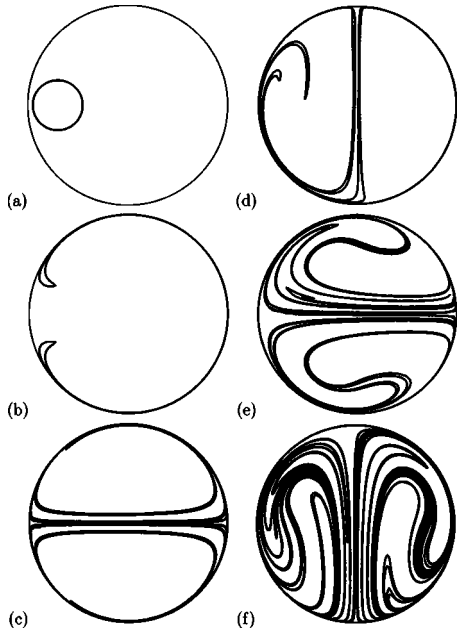

FIG. 5. Advection of dye by the dipole flow. Shown is the midplane cross section ($z=0$) of the boundary of a dyed fluid element. The x axis is horizontal and the y axis is vertical. The initial state (a) and stretching in steady dipole flow at $t=6$ (b) and $t=24$ (c). Stretching and folding in a time-periodic flow obtained by rotating its direction by 90° in the horizontal plane every six time units: the dyed element is shown at $t=12$ (d), $t=18$ (e), and $t=24$ (f). Time is measured in units of a/V.

In principle, the flow can also possess invariants related to dynamical rather than geometrical symmetries.[17] Such dynamical invariants, for instance, define the boundaries of integrable islands embedded in the chaotic sea of generic Hamiltonian systems and are often present in multicomponent chaotic flows in spherical droplets.[20–23] However, the importance of dynamical invariants is relatively small as they can be destroyed by simply changing the relative strength of the components of the flow. Therefore, in the following we will concentrate on the geometrical invariants which cannot be destroyed so easily, yet can often be found analytically without solving the equations of motion.

To begin with, consider the flow caused by a uniform horizontal temperature gradient for a droplet immersed in an unbounded substrate. The temperature gradient (we will take it to be in the x direction, see Fig. 4) will induce a dipole flow (1) inside the droplet with the axis $\mathbf{e}=\mathbf{e}_x$. The poor mixing properties of this flow can be demonstrated by following the motion of a small dyed fluid element inside the microdroplet [Figs. 5(a)–5(c)]. To determine the evolution of the dye the flow (1) is integrated forward in time starting from an initial condition shown in Fig. 5(a). The dye is stretched along the axis of the flow and the surface of the droplet within a single characteristic turnover time for the flow [Fig. 5(b)], but never spreads throughout the droplet, even after repeated stretching [Fig. 5(c)]. Poor mixing can be expected in this case because the steady dipole flow is effectively one dimensional (and, therefore, cannot be chaotic) because it possesses two invariants,[17]

$$I_d = \frac{z}{y}, \quad J_d = z^2(1-r^2), \tag{10}$$

related to the orientation of a plane containing the streamline and the stream function of the flow in that plane.

This result can be immediately generalized to droplets confined by straight microchannels. Even though the droplet in this case is not spherical, the flow is topologically identical to the dipole flow shown in Fig. 1. As a result no chaotic advection will result from recirculation of the liquid caused by translation of the droplet. The claims of apparent good mixing reported for this setup[28] rely on the experimental observations of the *depth-averaged* concentration which appears to be uniform, despite a strong inhomogeneity in three dimensions.

It is easy to see that the symmetry of the flow about the $y=0$ midplane of the droplet will prevent mixing between the left ($y>0$) and right ($y<0$) hemispheres of the droplet, even if the corrections to the dipole flow, such as the quadrupole flow (2), the Taylor flow (3) are included. Indeed, none of the streamlines can cross the symmetry plane of the flow, which serves as a barrier to transport between the left and right hemisphere in this case. This conclusion also applies to one dimensional motion of deformed (nonspherical) droplets confined either by channels with symmetric cross section[28,33] or by flat parallel surfaces.[29,31] This transport barrier can be broken and mixing between the two halves of the droplet achieved, by switching the direction of the flow, as was discovered by trial and error in electrowetting mixing studies.[30,31] Improved mixing in pressure-driven droplets moving through bent microchannels[33] is also due to direction switching of the recirculation flow.

Each flow invariant defines an infinite set of invariant surfaces, much like the $y=0$ symmetry plane. To realize complete mixing, all invariants of the flow must be destroyed. The time dependence of the flow introduced by switching the direction of the thermal gradient in the horizontal plane destroys the invariant I_d of the dipole flow (but not J_d). The resulting flow, therefore, becomes effectively three dimensional (two space variables plus time) and so chaotic dynamics becomes possible. Furthermore, direction switching introduces folding; repeated stretching and folding of the fluid elements by a time-periodic flow produces efficient stirring in the $z=0$ midplane of the droplet, as the results of numerical integration shown in Figs. 5(a) and 5(d)–5(f) demonstrate. This time-periodic flow can be thought of as a three dimensional version of the two dimensional Aref's blinking vortex.[5]

It is important to note that the presence of chaotic advection does not guarantee good mixing. Indeed, since the invariant J_d is not destroyed by direction switching, chaotic streamlines are confined to two dimensional surfaces of revolution defined by

$$x^2 + y^2 = 1 - z^2 - \frac{J_d}{z^2}, \tag{11}$$

as indicated by the intersections of a representative chaotic streamline with a fixed vertical midplane shown in Fig. 6(a). (Since the flow is formally four dimensional, its proper

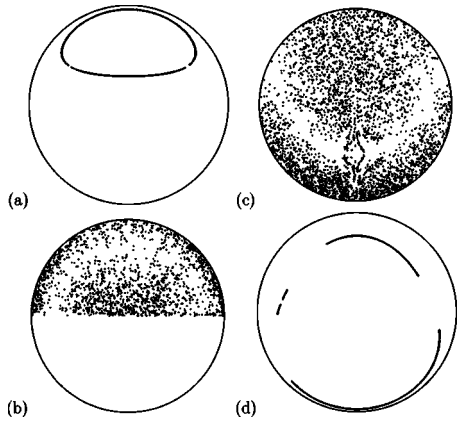

FIG. 6. Intersections of a chaotic streamline with the $x=0$ midplane of the droplet. The z axis is vertical. The flow is made time dependent by switching its direction by 120° every four time units. (a) Dipole flow. (b) Superposition of dipole and quadrupole flow. (c) Superposition of dipole, quadrupole and Taylor flow. (d) Superposition of dipole and Taylor flow. Parameters are chosen such that $\lambda=V_d=1$, $V_t=0.4$, $V_q=0.2$. The total time is $t_{\max}=8000$ (666 periods).

Poincaré section will be three dimensional rather than two dimensional.) Under the action of chaotic advection a dyed fluid element will only spread over thin shells defined by Eq. (11), where J_d varies over the values corresponding to the initially dyed region of the fluid. The same conclusions apply if the axis of the flow is rotated in a plane by arbitrary angles at arbitrary times (or if the axis oscillates periodically as proposed by Angilella and Brancher[24]). This result indicates that the symmetry of the pure dipole flow is so high that mixing will be incomplete even with the addition of time dependence.

The symmetry of the flow can be lowered by lowering the symmetry of the driving force, e.g., by making the temperature gradient nonuniform. For instance, a quadratic nonuniformity in the temperature field in the direction of the primary gradient, $T=T_0+\kappa_0 x+\kappa_1 x^2$, leads to a quadrupole correction (2) to the dipole flow with the same axis $\mathbf{e}=\mathbf{e}_x$. In this case the resulting steady flow is still axisymmetric and so again possesses two invariants. The stream function of the combined flow $\mathbf{v}=\mathbf{v}_d+\mathbf{v}_q$ allows us to easily find them:

$$I=\frac{z}{y}, \quad J=(V_d+2V_q x)z^2(1-r^2). \tag{12}$$

The addition of time dependence induced by switching the direction of the temperature gradient in the horizontal plane destroys both invariants (12) for almost all values of I and J. As a result, chaotic streamlines are no longer constrained to two-dimensional surfaces and thoroughly sample the droplet volume as Fig. 6(b) illustrates. However, a surface defined by $I=J=0$, namely, the midplane $z=0$, remains invariant with respect to rotations in the horizontal plane and prevents mixing between the top and bottom hemisphere of the microdroplet: the streamlines of the flow and hence the dye particles never cross the $z=0$ midplane. (If the time dependence of the flow is due to a periodic modulation of the quadrupole contribution, as is the case in the experimental setup studied by Ward and Homsy,[25] one still obtains chaotic mixing only in two dimensions as the invariant I in (12) is preserved.)

The final transport barrier is destroyed by the correction to the dipole/quadrupole flow induced by the shear in the substrate fluid. Unlike the dipole and quadrupole flows whose streamlines do not cross the midplane $z=0$ (see Figs. 1 and 2), the streamlines of the Taylor flow do cross that plane (see Fig. 3). As a result, the streamlines of the combined dipole/quadrupole/Taylor flow can also cross the midplane, enabling mixing between the top and bottom hemisphere as Fig. 6(c) illustrates.

It is important to note that the quadrupole flow contribution is essential for introducing chaotic advection in three dimensions. This can be seen by considering the combination of the dipole and Taylor flows alone. Since Taylor flow has the same symmetry with respect to the plane $x=0$ as the dipole flow (compare Figs. 1 and 3) and both flows are time reversible (as is every Stokes flow), all trajectories of the Taylor flow are closed. This, in turn, means that Taylor flow also possesses two invariants. These invariants, however, are not as easy to find, since Taylor flow is not axially symmetric and hence one cannot use the stream function of the flow. The invariants can nevertheless be found directly from their definition, $\mathbf{v}_t\cdot\nabla J_t=0$. Solving the resulting partial differential equation one finds both invariants:

$$\begin{aligned} I_t &= y^3(1-r^2), \\ J_t &= (\lambda+1+2z^2-r^2)^{3/2}(1-r^2). \end{aligned} \tag{13}$$

Again the first flow invariant is destroyed by rotations in the horizontal plane, while the second invariant is preserved. This is a consequence of a general statement which can be easily proven: any time-reversible flow $\mathbf{v}$ such that

$$\begin{aligned} v_x(-x,y,z) &= v_x(x,y,z), \\ v_y(-x,y,z) &= -v_y(x,y,z), \\ v_z(-x,y,z) &= -v_z(x,y,z) \end{aligned} \tag{14}$$

possesses at least one invariant which is preserved under rotations in the xy plane. This statement follows directly from the symmetry of the closed orbits of such flows about the $x=0$ plane. In particular, the superposition of the dipole and Taylor flow has an invariant which is preserved under rotations. In the limit $\lambda\to\infty$ it takes a simple form:

$$J=(V_t-V_d z)^2(1-r^2). \tag{15}$$

The corresponding time-periodic flow whose direction is switched in the horizontal plane again has poor mixing properties: although its streamlines are chaotic, they are constrained to two-dimensional surfaces of revolution defined by the remaining invariant. The cross section of such a surface is shown in Fig. 6(d). This result also proves the numerical conclusion of Bryden and Brenner[26] that the superposition of the (steady) dipole and Taylor flow is nonchaotic when the vorticity vector of the shear flow is orthogonal to the axis of the dipole flow.

Summing up, we have shown that all geometrical invariants of the flow inside a droplet can be broken by immersing

it in a layer of substrate fluid with a free surface and driving it using a thermal gradient whose direction is periodically switched in a horizontal plane. The destruction of flow invariants removes the transport barriers inside the droplet, thereby facilitating quick and thorough mixing.

V. CONCLUSIONS

The analysis presented above should have broad applicability. On the most general level, one concludes that the existence and number of invariants play a crucial role in determining the mixing properties of the flow. In particular, in order to achieve full three dimensional mixing the flow within the droplet should be designed to destroy all invariant surfaces in the interior of the droplet. As the example with the dipole/Taylor flow combination shows, destroying the simple geometrical symmetries of the flow (e.g., making the combined flow nonaxisymmetric) might not be sufficient for complete mixing. In this sense the flow invariants provide a more useful way of characterizing the mixing properties of the flow than its symmetries.

More specifically, the types of flows that we have considered (dipole, quadrupole, and Taylor flow) are the most common types of interior flows arising inside spherical microdroplets, regardless of the nature of driving forces. That is not surprising as they merely represent the first few terms in the Lamb's general solution. Therefore, many details of our analysis should be directly applicable to situations when microflows are driven by, e.g., external shear, buoyancy, or electrical fields. Furthermore, many of the results we have obtained for spherical droplets should naturally generalize to deformed shapes such as liquid plugs in microchannels with cylindrical or rectangular cross section[28,33] or droplets compressed between two parallel planes.[30–32] The flows inside these shapes are topologically similar to flows in spherical microdroplets and therefore should have similar mixing properties, at least in steady state.

Finally, our results suggest that once the geometrical invariants in a nonperturbative time-dependent flow are destroyed, one obtains extremely thorough mixing in the full volume of the droplet. This is likely due to the fact that the resulting flow is effectively four dimensional. It is also possible to obtain such thorough mixing in some nonperturbative composite steady flows[21,22] (in fact the steady dipole/quadrupole/Taylor flow is also chaotic!), however thorough mixing requires carefully choosing the relative strength of different components. The mixing uniformity of our time-periodic flow is not perfect—there are shell-like regions [see Figs. 6(b) and 6(c)] which are visited by chaotic trajectories less frequently. This is a generic feature observed in most chaotic flows, steady or time periodic, and its origin is currently under investigation.

[1] G. M. Whitesides and A. D. Stroock, "Flexible methods for microfluidics," Phys. Today **54** (6), 42 (2001).
[2] L. Bousse, C. Cohen, T. Nikiforov, A. Chow, A. R. Kopf-Sill, R. Dubrow, and J. W. Parce, "Electrokinetically controlled microfluidic analysis systems," Annu. Rev. Biophys. Biomol. Struct. **29**, 155 (2000).
[3] M. Burns, C. Mastrangelo, T. Sammarco, F. Man, J. Webster, B. Johnson, B. Foerster, D. Jones, Y. Fields, A. Kaiser, and D. Burke, "Microfabricated structures for integrated DNA analysis," Proc. Natl. Acad. Sci. U.S.A. **93**, 5556 (1996).
[4] T. S. Sammarco and M. A. Burns, "Thermocapillary pumping of discrete drops in microfabricated analysis devices," AIChE J. **45**, 350 (1999).
[5] H. Aref, "Stirring by chaotic advection," J. Fluid Mech. **143**, 1 (1984).
[6] J. M. Ottino, *The Kinematics of Mixing: Stretching, Chaos, and Transport* (Cambridge University Press, Cambridge, 1989).
[7] R. H. Liu, M. A. Stremler, K. V. Sharp, M. G. Olsen, J. G. Santiago, R. J. Adrian, H. Aref, and D. J. Beebe, "Passive mixing in a three-dimensional serpentine microchannel," J. Microelectromech. Syst. **9**, 190 (2000).
[8] A. D. Stroock, S. K. W. Dertinger, A. Ajdari, I. Mezic, H. A. Stone, and G. M. Whitesides, "Chaotic mixer for microchannels," Science **295**, 647 (2002).
[9] A. A. Darhuber, J. P. Valentino, J. M. Davis, S. M. Troian, and S. Wagner, "Microfluidic actuation by modulation of surface stresses," Appl. Phys. Lett. **82**, 657 (2003).
[10] M. G. Pollack, R. B. Fair, and A. D. Shenderov, "Electrowetting-based actuation of liquid droplets for microfluidic applications," Appl. Phys. Lett. **77**, 1725 (2000).
[11] S. K. Cho, H. Moon, and C.-J. Kim, "Creating, transporting, cutting, and merging liquid droplets by electrowetting-based actuation for digital microfluidic circuits," J. Microelectromech. Syst. **12**, 70 (2003).
[12] J. S. Hadamard, "Mouvement permenent lent d'une sphere liquide et visqueuse dans un liquide visqueux," C.R. Acad. Sci., Ser. IIc: Chim **152**, 1735 (1911).
[13] N. O. Young, J. S. Goldstein, and M. J. Block, "The motions of bubbles in a vertical temperature gradient," J. Fluid Mech. **6**, 350 (1959).
[14] S. M. Lee, D. J. Im, and I. S. Kang, "Circulating flows inside a drop under time-periodic nonuniform electric fields," Phys. Fluids **12**, 1899 (2000).
[15] G. I. Taylor, "The viscosity of a fluid containing small drops of another fluid," Proc. R. Soc. London, Ser. A **138**, 41 (1932).
[16] G. I. Taylor, "Studies in electrohydrodynamics I. The circulation in a drop by an electric field," Proc. R. Soc. London, Ser. A **291**, 159 (1966).
[17] I. Mezic and S. Wiggins, "On the integrability and perturbation of three-dimensional fluid flows with symmetry," J. Nonlinear Sci. **4**, 157 (1994).
[18] D. L. Vainshtein, A. A. Vasiliev, and A. I. Neishtadt, "Changes in the adiabatic invariants and streamline chaos in confined incompressible Stokes flow," Chaos **6**, 67 (1996).
[19] A. I. Neishtadt, D. L. Vainshtein, and A. A. Vasiliev, "Chaotic advection in a cubic Stokes flow," Physica D **111**, 227 (1998).
[20] D. Kroujiline and H. A. Stone, "Chaotic streamlines in steady bounded three-dimensional Stokes flows," Physica D **130**, 105 (1999).
[21] K. Bajer and H. K. Moffatt, "On the class of steady confined Stokes flows with chaotic streamlines," J. Fluid Mech. **212**, 337 (1990).
[22] H. A. Stone, A. Nadim, and S. H. Strogatz, "Chaotic streamlines inside drops immersed in steady Stokes flows," J. Fluid Mech. **232**, 629 (1991).
[23] J. H. E. Cartwright, M. Feingold, and O. Piro, "Chaotic advection in three-dimensional unsteady incompressible laminar flow," J. Fluid Mech. **316**, 259 (1996).
[24] J. R. Angilella and J. P. Brancher, "Note on chaotic advection in an oscillating drop," Phys. Fluids **15**, 261 (2003).
[25] T. Ward and G. M. Homsy, "Electrohydrodynamically driven chaotic mixing in a translating drop," Phys. Fluids **13**, 3521 (2001).
[26] M. D. Bryden and H. Brenner, "Mass-transfer enhancement via chaotic laminar flow within a droplet," J. Fluid Mech. **379**, 319 (1999).
[27] T. Ward and G. M. Homsy, "Electohydrodynamically driven chaotic mixing in a translating drop. II. Experiments," Phys. Fluids **15**, 2987 (2003).
[28] K. Hosokawa, T. Fujii, and I. Endo, "Handling of picoliter liquid samples in a poly(dimethylsiloxane)-based microfluidic device," Anal. Chem. **71**, 4781 (1999).
[29] P. Paik, V. K. Pamula, M. G. Pollack, and R. B. Fair, "Electrowetting-based droplet mixers for microfluidic systems," Lab Chip **3**, 28 (2003).
[30] P. Paik, V. K. Pamula, M. G. Pollack, and R. B. Fair, "Rapid droplet mixers for digital microfluidic systems," Lab Chip **4**, 253 (2003).
[31] J. Fowler, H. Moon, and C.-J. Kim, "Enhancement of mixing by droplet-based microfluidics," Proceedings of the 15th IEEE Conference on Micro-ElectroMechanical Systems 2002, Las Vegas, NV.
[32] T. Taniguchi, T. Torii, and T. Higuchi, "Microchemical reactor in micro droplets—electrostatic manipulation of micro droplets," Proceedings of the International Symposium on Microchemistry and Microsystems 2001, Kawasaki, Japan.

[33]H. Song, J. D. Tice, and R. F. Ismagilov, "A microfluidic system for controlling reaction networks in time," Angew. Chem., Int. Ed. **42**, 768 (2003).
[34]D. E. Kataoka and S. M. Troian, "Patterning liquid flow on the microscopic scale," Nature (London) **402**, 794 (1999).
[35]N. Garnier, R. O. Grigoriev, and M. F. Schatz, "Optical manipulation of microscale fluid flow," Phys. Rev. Lett. **91**, 054501 (2003).
[36]H. Brenner, "The Stokes resistance of a slightly deformed sphere," Chem. Eng. Sci. **19**, 519 (1964).
[37]S. H. Chen, "Movement of a fluid sphere in the vicinity of a flat plane with constant temperature gradient," J. Colloid Interface Sci. **230**, 157 (2000).